TRACER TRANSPORT IN THE NASA-AMES GCM.

S. M. Nelli, *Department of Astronomy, New Mexico State University, Las Cruces, NM, 88001, USA (snelli@nmsu.edu),* **J. R. Murphy,** *NMSU, Las Cruces, NM, USA (murphy@nmsu.edu),* **A. L. Sprague**, *LPL, UofA, Tucson, AZ, USA (sprague@lpl.arizona.edu),* **W. C. Feldman**, *LANL, Los Alamos, NM, USA (wfeldman@lanl.gov),* **T. H. Prettyman,** *LANL, Los Alamos, NM, USA (thp@lanl.gov),* **W. V. Boynton,** *LPL, UofA, Tucson, AZ, USA (wboynton@lpl.arizona.edu).*

Introduction:

Atmospheric dust, water vapor/ice, and minor gas species (argon, nitrogen) are known as tracers of the martian atmosphere. Their abundance by mass is negligible, with nitrogen being the largest contributor at ~2.5% [1]. They can be used to track the atmospheric circulation. Studying tracers with a General Circulation Model (GCM) helps in the understanding of what dynamical processes are producing the current martian circulation. Studying how well the model reproduces tracer fields compared to observations produces a diagnostic test of how well model dynamics/circulation reproduce actual processes on Mars. Through statistical analysis of the space and time domain of the tracer field one can decompose the atmospheric circulation into its three main components, the zonal mean circulation, stationary and transient eddies [2].

Ideally, you want a tracer with no source or sink so that its abundance at a given location at any time is due solely to atmospheric circulation without the complications of having to deconvolve the effects of a source or sink. In this regard, argon and nitrogen are perfect for such studies. But, only the most recent Odyssey data sets have allowed the community to utilize the potential of such tracers. Much of the previous research has been done using dust and water vapor/ice as tracers, in which a great deal more data is available [3,4]. These tracers have sources and sinks, which can create problems in separating the physics from the dynamics.

The last few years have been spent studying how effectively the NASA-Ames General Circulation Model captures the martian circulatory dynamics by trying to match tracer transport in the model to observed data. Tracers in the GCM are carried as mass mixing ratios. The tracer field is three-dimensional in space and tracer transport is determined by the solution to the continuity equation, which accounts for advection, diffusion, and source and sink terms. Dust and water ice have the added element of gravitational settling. The Ames-GCM makes use of the ARIES/GEOS dynamical core developed at Goddard Space Flight Center [5] to solve the continuity equation.

Studying tracer transport in the model to test the accuracy in which the GCM captures martian dynamics has led to valuable secondary scientific gains. Current science includes determining the main factors driving the asymmetric enhancement of argon between the poles [6] and possible atmospheric recharge of the equatorial water equivalent hydrogen-rich regions [7]. Discerning the sensitivity of the dust cycle to changes in the water cycle in a fully coupled simulation is just beginning to be researched. Initial results show potential.

Non-condensable gases:

Data. More than one martian year of atmospheric argon measurements from the 2001 Mars Odyssey Gamma Ray Spectrometer (GRS) [8] have been reduced for analysis. The data investigated by the authors commence on $L_s = 21.95^\circ$ (June, 2002) and end with data taken at $L_s = 60^\circ$ (November, 2004) the following Mars year (~1.1 Mars years later). Of particular interest in these data are the enhanced absolute and relative abundances of atmospheric argon at polar latitudes during the winter season compared to the observed atmospheric argon abundance at lower latitudes (Fig. 1). The GRS data indicate a 6-fold enhancement in argon abundance at the south pole and a 3-fold enhancement at the north pole [6,9] compared to argon mixing ratio values measured with the Viking Lander 2 Gas Chromatograph Mass Spectrometer at northern middle latitudes during northern summer [1] in 1976.

Model Application. Non-condensable gases such as argon and nitrogen in the martian atmosphere are truly passive tracers; they are highly unreactive gases with no known sources or sinks on annual or decadal time scales. Only CO_2 condensation, and the subsequent transport of this CO_2-depleted atmosphere and its mixing with non-depleted air, can change the local non-condensable gas mixing ratio. This makes argon an ideal tracer for studying atmospheric dynamics [6]. For this investigation, the NASA-Ames Mars GCM [10,11,12,13] has been employed to investigate the observed argon enhancement values. The modeling work permits determination of the factors controlling the magnitudes of the observed argon enhancement and permits exploration of the sensitivity of the enhancement to hemispherically dependent conditions (topography, season of orbital perihelion, etc.), in an attempt to understand the hemispheric asymmetry in observed argon enhancement.

Set up. We initialize the model with a passive tracer (representing the non-condensing gas) in the

form of a spatially uniform mass mixing ratio. The tracer has no source or sink; only advection and CO_2 condensation change the local mixing ratio. The initial mixing ratio is specified to be 4.7% based on Viking Lander 2 GCMS measurements [1]. A different value would change the absolute abundances discussed, but would not affect the relative enhancement values. The model is initialized with an amount of atmospheric CO_2 that will produce an annual pressure cycle representative of the VL1 measurements [14] at the grid point nearest the VL1 location in the model. With the CO_2 surface ice accumulation agreeing with Neutron Spectrometer data [15,16] and the simulated pressure cycle near the VL1 position similar to that observed, there is confidence that the total amount of condensed CO_2 is appropriate and thus the modeled enhancement values are not being seriously affected by too little or too much CO_2 condensation.

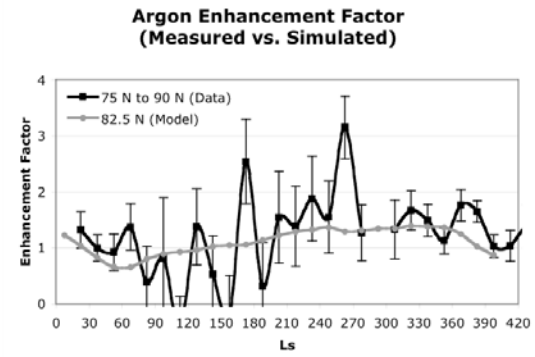

Figure 1a&b: Enhancement of argon at the north and south pole above the measured value taken at the VL2 site for $L_s = 135^\circ$. Model and data derived values are overlaid for comparative purposes. The model is qualitatively consistent with observed values.

Results. Initializing the GCM with parameters to simulate current martian conditions reproduces relative non-condensable abundances at the grid point nearest the VL2 site that match the GCMS measurements. This suggests that the model captures the global scale circulation. The model produces a non-condensable gas enhancement that is asymmetric in magnitude between the south and north pole (figure 1, both panels). This asymmetry qualitatively fits the observed data derived from GRS. In both the data and the model, argon enhancement increases smoothly as a function of L_s over the south polar region during southern hemisphere fall and recedes in the winter. High frequency oscillations in the enhancement occurring at L_s~60˚, 120˚, and 150˚ are not matched by the model. The argon enhancement in the model at the south pole is a factor of two less than the data, suggesting that mixing off this pole in the GCM is too strong by a factor of two (figure 1, bottom panel). Enhancement in the north during northern winter is much less pronounced and much less regular in formation than in the south in both the model and the data. Despite the wildly varying magnitude of the argon enhancement derived by GRS in the north, the simulated magnitudes for argon enhancement fall within the error bars (figure 1, top panel). Here, also, the model is unable to match the high frequency oscillations in the data (which are much more pronounced in the north). These high frequency oscillations in the north polar enhancement have a longer period than the strong weather systems that form in the lowlands of Acidalia and Utopia/Arcadia [17,18]. The source of these oscillations is still not well understood.

Water Cycle:

Data. The two definitive data sets on water vapor abundance on Mars are those obtained during two major orbiter missions: the Viking Orbiters in the late 1970's with their Mars Atmospheric Water Detector (MAWD) [19], and Mars Global Surveyor from 1997 to present with its Thermal Emission Spectrometer (TES) [3,20]. Additionally, the Mars Odyssey Neutron Spectrometer (NS) and the Gamma Subsystem (GS) provide the first ever data set of the surface distribution of (water-equivalent) hydrogen [21,22,23,24,25].

Martian surface water ice deposits at the north pole is well known [26]. Surface and subsurface water ice is thermodynamically stable poleward of ~45˚ latitude [27]. The interpretation of Odyssey data, which places 50% to 70% by mass WEH in the upper one meter of the regolith at both poles, is expected. The real surprise is the detection of low latitude reservoirs in Arabia and the western flanks of Tharsis containing between 2% and 10% WEH [7,25] by mass in the upper one meter of the regolith. Since near-surface ice is expected to be thermodynamically unstable, these regions are presumed to be populated by hydrated minerals [28]. However, the possibility of water ice from a previous epoch covered by a low-permeability layer of dust cannot be overlooked [29].

Model Application: The origin of the equatorial

hydrogen reservoirs is disputed. The reservoirs lie along a constant topographic contour of zero km [25]. The constant topographic altitude may be the result of an exposed water table fed by the water ice cap located over the south pole [30]. If so, then how does one explain the water rich regions near Solis Planum and Xanthe Terrae, which due to their high altitude, are inaccessible from the major water reservoirs at Arabia Terra and Medusae Fossae (figure 2) [30]. One plausible solution for recharge of these areas is via the atmosphere.

Modeling work with the Ames GCM investigates the possibility that the observed WEH can be recharged via current climate conditions. Preliminary correlations between the deposition pattern of water ice in the model and the WEH-rich equatorial regions seen by NS are promising (figure 3). Further investigation is ongoing into the importance the North/South Pole water ice cap (how they control atmospheric water abundance), cloud particle fall speed, and Hadley circulation have in regard to the correlation between the spatial pattern of the water deposition in the model and the WEH-rich equatorial regions on Mars. Near-surface water vapor abundances in the model and knowledge of mineral properties can be used to calculate hydration rates in the WEH-rich equatorial regions to obtain an estimate of the lifespan of these regions. This work is currently in progress.

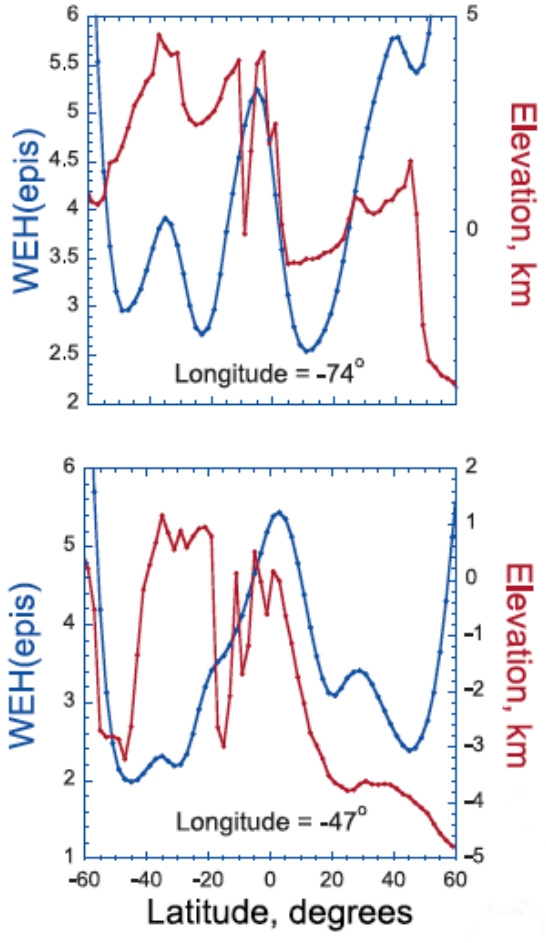

Figure 2: Meridional cuts through topography (red) and WEH abundance (blue) for two longitudes crossing Valles Marineris. This region cannot be hydrated by a south polar ice cap fed water table because the canyons of Valles Marineris cut off these high altitude regions. [7]

Set-up. The model is run with input parameters appropriately set to give a water and dust cycle representative of TES results [31] (within a factor of 2). These parameters include the surface stress lifting threshold for dust [32] and dust devil lifting [33], sublimation rate of water ice [34], and cloud particle size [35]. A full water cycle is employed in the model. This full cycle includes the sublimation of water ice off a reservoir or from sites of deposition through the calculation of a sublimation flux rate [34]. Supersaturated water condenses to form cloud particles [35]. The amount of supersaturated water and the number of condensation nuclei (dust) determine the size and number of cloud particles. However, the dust is not incorporated into the cloud particle. Particle fall speeds are calculated using the Stokes relationship. The Cunningham slip-flow correction factor is included to account for particles smaller than the mean free path of CO_2 molecules being able to fall quicker than allowed by Stokes relationship [36].

Results. Initializing the GCM to match current climate conditions on Mars produces a workable water cycle. Maximum water vapor abundance over both poles is 70% of that derived from TES spectra [3,20]. However, the northern hemisphere mid-latitude local maximum water vapor abundance during northern winter is a factor of two too wet. As with the argon cycle, water vapor appears to be mixed too vigorously off the south polar cap. Water vapor maxima/minima in the atmosphere occur seasonally in accordance with observed data. The model produces an aphelion water ice cloud belt in the northern sub-tropics. The clouds form at a height of ~10 km and have a seasonal extent consistent with that derived from TES spectra [7].

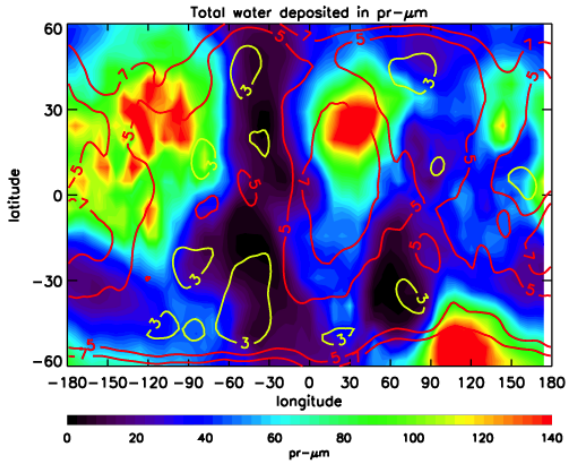

Figure 3: Contours are WEH abundance for 3, 5, & 7% by

mass as measured by the Neutron Spectrometer on board Odyssey. The color shading is the annual water ice deposition upon the surface from the atmosphere simulated by the model. The deposition is not net accumulation. The water ice sublimates away during the daylight hours.

At night, in the model, air in contact with the ground cools via conduction and radiation and flows down the slope of the topography. Upon reaching the condensation temperature, this moisture-laidened air produces a ground fog and precipitates onto the surface [37]. At equatorial and mid-latitudes, the coldest near-surface temperatures occur at longitudes of lowest thermal inertia and highest surface elevation. A wave number two longitudinal pattern of deposition occurs in the model over Arabia and Tharsis. Relative minima of water deposition occur in longitudes of topographic lows such as Acidalia, Chryse, and Argyre in the west, and Utopia, Isidis, and Hellas in the east [7].

Coupled Water and Dust Cycle:

Data. Regional dust storms on Mars occur at a rate of several per year, but planet-encircling dust storms occur infrequently [38]. Statistics for the frequency of planet-encircling dust storms are low. Without an orbiting spacecraft, observations can only be made from Earth when Mars is at opposition [39,40]. The last 100 years of ground-based observation yields global dust storms on Mars roughly every 4 martian years [41].

Model Application. The ability for GCMs to produce variable and spontaneous dust storms is a unique problem in the modeling community. Historically, long duration simulations of the dust cycle show little yearly variation in the patterns of dust lifting and sedimentation [12,13]. Basu et al. [42] have made recent strides in resolving this issue by inducing a spontaneous dust storm, but details are not yet available. These models typically have decoupled the dust and water cycles. Cloud formation does not lead to dust removal from the atmosphere; doing so affects the vertical distribution, heights obtained and sedimentation times of the dust particles, and thus, the temperature.

Modeling of a coupled cycle is important in aiding our interpretation of observed data. Sensitivity studies on how one cycle affects the other have yet to be undertaken. With the use of the Ames GCM, research has started on determining the sensitivity of the water and dust cycle when coupled to each other. This project studies the annual and interannual variability of one cycle (water/dust) due to perturbations in the other (dust/water). Through the interaction of cloud formation, changes in the source and sink of both aerosols are studied. This project also analyzes the changes in the horizontal and vertical distribution of both aerosols and how these changes lead to interannual variability within the model.

Set-up. An initial decoupled simulation is run to spin-up the model and obtain a representative dust and water cycle based upon TES observations. A full water cycle (as mentioned in the previous section on the water cycle) is employed as well as interactive dust lifting. Dust is lifted via a surface stress parameterization [32] and dust devil lifting parameterization [33]. When coupled, dust is incorporated into water-ice cloud particles when clouds form. Dust either returns to the atmosphere when clouds evaporate upon reaching an unsaturated layer, or fall to the ground at their calculated fall speed. Initial simulations do not treat the radiative effects of cloud particles, nor of the dust nuclei in the cloud particles. These processes will be tackled once the initial sensitivities of the two coupled cycles have been explored.

Results. Initial results are promising, as dust and water cycles during northern spring and summer, when energy (and dust) input into the system is lowest, match TES observation. The dust cycle spirals out of control during late northern fall and the planet becomes enshrouded with dust. Subsequent work needs to be done to understand why.

Discussion:

This work is a study of the effectiveness of tracer transport in the Ames GCM. The overall characterization by the model of the global scale transport is good. The model obtains seasonal variation of tracers in good comparison with observed data. Tracer transport off the south pole is too vigorous and the high frequency oscillations in the argon enhancement data is not reproduced in the model. A coupled water and dust cycle in the model produces similar cycles to those found in TES spectra for northern spring and summer but cannot yet produce a realistic cycle over one full martian year.

Reference:

[1] Owen, T., et al., (1977) *JGR*, **82**, 4635-4639. [2] Peixoto, J.P. & A.H. Oort, (1992), *Physics of Climate*. [3] Smith, M.D., (2004), *Icarus*, **167**, 148-167. [4] Clancy, R.T. et al., (1996), *Icarus*, **122**, 36-62. [5] Suarez, M.J. & L.T. Takacs (1995) NASA Technical Memorandum 104606, Vol. 5. [6] Sprague, A.L., et al., (2005), *JGR*, Mars atmospheric argon: tracer for understanding Martian circulation and dynamics, submitted. [7] Feldman, W.C., et al., (2005), *JGR*, Topographic control of hydrogen deposits at low latitudes to mid-latitudes of Mars, in press. [8] Boynton, W.V., et al., (2004), *Space Sci. Rev.*, **110**, 37-83. [9] Sprague, A.L., et al., (2004), *JGR*, **104**, 8957-8974. [10] Haberle, R.M., et al., (1999), *Icarus*, **50**, 322-367. [11] Haberle, R.M., J.R. Murphy, & J. Schaeffer, (2003), *Icarus*, **161**, 66-89. [12] Kahre, M.A., et al., (2005), *GRL*, **32**, L20204 [13] Kahre, M.A., J.R. Murphy, & R.M. Haberle, (2005), *JGR*, Modeling the martian dust cycle and surface dust reservoirs with the NASA Ames GCM, submitted. [14] Hess, S.L., et al., (1980), *GRL*, **7**, 197-200. [15] Feldman, W.C., et al., (2003), *JGR*, **108**, doi:10.1029/2003JE002101. [16] Prettyman, T.H., et al., (2004), *JGR*, **109**, doi:10.1029/2003JE002139. [17] Barnes, J.R., (2003), *6th Inter. Mars Conf.*, **3127**. [18] Banfield, D., et al., (2004), *Icarus*, **170**,

365-403. [19] Federova, A.A., A.V. Rodin, & I.V. Baklanova, (2004), *Icarus*, **171**, 54-67. [20] Smith, M.D., (2002), *JGR*, **107**, doi:10.1029/2001JE001522 [21] Boynton, W.V., et al., (2002), *Science*, **297**, 81-85. [22] Feldman, W.C., et al., (2002), *Science*, **297**, 75-78. [23] Mitrofanov, I., et al., (2002), *Science*, **297**, 78-81. [24] Boynton, W.V., et al., (2005), *JGR*, Data Analysis of the GRS GS instrument, submitted. [25] Feldman, W.C., et al., (2004), *JGR*, **109**, doi:10.1029/2003JE002160. [26] Snyder, C.W., (1979), *JGR*, **84**, 8487-8519. [27] Mellon, M.T., & B.M. Jakosky, (1993), *JGR*, **98**, 3345-3364. [28] Feldman, W.C., et al., (2004), *GRL*, **31**, doi:10.1029/2004GL020181. [29] Mischna, M.A., & M.I. Richardson, (2005), *GRL*, **32**, doi:10.1029/2004GL021865. [30] Feldman, W.C., et al., (2004), *GRL*, **31**, doi:10.1029/2004GL020661. [31] Smith, M.D., et al., (2002), *JGR*, **106**, 23929-23946. [32] Newman, C.E., S.R. Lewis, & P.L. Read, (2005), *Icarus*, **174**,135-160. [33] Newman, C.E., et al., (2002), *JGR*, **107**, doi:10.1029/2002JE001910. [34] Haberle, R.M., & B.M. Jakosky, (1990), *JGR*, **95**, 1423-1437. [35] Montmessin, F., et al., (2004), *JGR*, **109**, doi:10.1029/2004JE002284. [36] Pruppacher, H.R., & J.D. Klett, (2000), *Microphysics of Clouds and Preicipitation*, 416 pp. [37] Wilson, R.J., & M.D. Smith, (2005), *LPSC XXXVI*, #1947. [38] Cantor, B.A., et al., (2001), *JGR*, **106**, 23653-23687. [39] Read, P.L., & S.R. Lewis, (2004), *The Martian Climate Revisited*, 202 pp. [40] Kahre, M.A., et al., (2005), *Icarus*, **179**, 55-62. [41] Martin, T.Z., & R.W. Zurek, (1993), *JGR*, **98**, 3221-3246. [42] Basu, S., M.I. Richardson, & R. J. Wilson, (2004), *JGR*, **109**, doi:10.1029/2004JE002243.